A new optical parametric amplifier based on lithium thioindate used for sum frequency generation vibrational spectroscopic studies of the Amide I mode of an interfacial model peptide

Roger L. York[1,†], George J. Holinga[1], Dean R. Guyer[2], Keith R. McCrea[3], Robert S. Ward[3], Gabor A. Somorjai[1,*]

[1]*Department of Chemistry, University of California, Berkeley, Berkeley, CA 94720 and Materials Science Division, Lawrence Berkeley National Laboratories, Berkeley, CA 94720*

[2]*LaserVision, Bellevue, WA 98004*

[3]*The Polymer Technology Group, Berkeley, CA 94710*

*Corresponding author: somorjai@berkeley.edu

[†]Current Address of this author: Department of Chemistry and Chemical Biology, Harvard University, Cambridge, MA 02138

Abstract

We describe a new optical parametric amplifier (OPA) that employs lithium thioindate, $LiInS_2$ (LIS), to create tunable infrared light between 1500 cm^{-1} and 2000 cm^{-1}. The OPA based on LIS described within provides intense infrared light with a good beam profile relative to similar OPAs built on silver gallium sulfide, $AgGaS_2$ (AGS), or silver gallium selenide, $AgGaSe_2$ (AGSe). We have used the new LIS OPA to perform surface-specific sum frequency generation (SFG) vibrational spectroscopy of the Amide I vibrational mode of a model peptide at the hydrophobic deuterated polystyrene (d_8-PS)/ phosphate buffered saline interface. This model polypeptide (which is known to be an α-helix in the bulk solution under the high ionic strength conditions employed here) contains hydrophobic leucyl (L) residues and hydrophilic lysyl (K) residues, with sequence Ac-LKKLLKLLKKLKL-NH_2. The Amide I mode at the d_8-PS/buffer interface was found to be centered around 1655 cm^{-1}. This can be interpreted as the peptide having maintained its α-helical structure when adsorbed on the hydrophobic surface, although other interpretations are discussed.

Introduction

The interaction of biological molecules with solid surfaces has important consequences for the biomaterial community, in addition to being an open and fundamental scientific problem.[1-3] It is well understood that a protein or peptide can denature as it adsorbs onto a solid surface (i.e. secondary structure is changed or often completely lost).[4] However, measuring the change in secondary structure at the molecular level when a protein or polypeptide adsorbs onto a solid surface has proven difficult in part due to a lack of surface specific techniques.

In recent years, several groups have turned to surface-specific sum frequency generation (SFG) vibrational spectroscopy to probe the interfacial structure of proteins and peptides with solid surfaces.[5-7] In this letter, we present a new type of optical parametric amplifier (OPA) based on lithium thioindate, $LiInS_2$ (LIS),[8, 9] which more easily allows for the creation of intense infrared light in the spectral window 1500 cm^{-1} to 2000 cm^{-1}. This allows for the SFG measurement the backbone Amide I mode (usually somewhere between 1600 cm^{-1} and 1700 cm^{-1}). The frequency of this mode is sensitive to the secondary structure of interfacial peptides.[10] For example, it is generally accepted in infrared and Raman spectroscopy that an Amide I mode observed around 1650 cm^{-1} is characteristic of an α-helix; whereas a β-sheet has a characteristic Amide I mode observed at 1630 cm^{-1} and 1690 cm^{-1}.[10] The Amide I mode of a random coil, however, can arise at any frequency in this spectral window.

Although many SFG studies of biomolecules at surfaces have focused on the spectral window 2800-3100 cm^{-1}, Chen and coworkers have been studying the Amide I vibrational mode of interfacial proteins and peptides since 2003.[11-14] In one of their

pioneering studies[13] they show that, much like in infrared and Raman spectroscopies, the frequency of the Amide I mode is sensitive to peptide secondary structure. In this study, they show that the Amide I mode of an α-helical peptide (in solution) at a hydrophobic surface (measured by SFG) is mainly observed as a single peak centered around 1650 cm^{-1}.

In this report, we present the study of the interfacial Amide I mode of a model peptide, the LK_{14} peptide, which is composed of hydrophobic leucine (L) and lysine (K) residues using a new type of OPA based on a LIS crystal.[15-17] This peptide is known to fold into an α-helix in solution if the ionic strength of the solution is sufficiently high.[15, 18] We have found that the frequency of the interfacial Amide I mode (measured by SFG) at the hydrophobic deuterated polystyrene (d_8-PS)/phosphate buffered saline (PBS) interface is 1655 cm^{-1}. Furthermore, we interpret the frequency of this interfacial Amide I mode to be characteristic of an α-helix. In the case of the peptide adsorbing from a high ionic strength solution, this is not unexpected: the results imply that the interfacial structure of this peptide is maintained upon adsorption. However, the assignment of this mode to a α-helix is not definitive, as discussed below.

Experimental

Sum Frequency Generation

SFG is based on a second-order non-linear process whereby two beams are overlapped in space and time on a surface and the resultant light at the sum-frequency is measured. In picosecond infrared-visible SFG, the two beams can be created by pumping a series of non-linear crystals by the 1064 nm fundamental of a Nd:YAG laser (in this

paper, we used a Continuum Leopard D-20 to measure the damage threshold of LIS, and the data in Figures 2, 3, and 4 were from an Ekspla PL2143A). In our set-up, the visible (532 nm) is the second harmonic of this fundamental. The tunable infrared is created by sending a portion of the 532 nm light into a tunable optical parametric generator (OPG) consisting of two KTP crystals. The OPG creates two tunable beams (~900 and ~1300 nm) of which one (~1300 nm) is sent to the OPA stage (where difference frequency generation (DFG) occurs-OPA and DFG are synonymous[19]), where it is mixed with the remaining 1064 nm light. This OPA stage often is composed of KTA or $LiNbO_3$ crystals, which provide strong conversion efficiencies out to the ~5 µm transparency limit of these oxides. Our prior choice of nonlinear crystals suitable for generation of deeper mid-infrared wavelengths has been limited primarily to two ternary chalcogenide semiconductor crystals, $AgGaSe_2$ (AGSe) or $AgGaS_2$ (AGS). AGS has sufficient birefringence and transparency to directly convert the Nd:YAG fundamental into tunable mid-IR out to ~9 µm, but the intrinsic damage threshold is low and the surface degrades rapidly with use. AGSe does not have this surface degradation problem but its use is limited to difference-frequency mixing the signal and idler outputs of a near infrared OPA, since it is not phase-matchable with a 1064 nm pump. For both crystals, these limitations result in mid-IR pulse energies that are low and not well suited for SFG vibrational spectroscopy. For the present study, we have incorporated the new nonlinear crystal, LIS, to replace the oxide crystals in our 1064 nm OPA. Figure 1 shows a schematic layout of the OPG/OPA system.

LIS has distinct advantages for mid-IR generation. The crystal possesses a transparency that spans from the visible out to 10 µm, a large birefringence that allows

phase-matching over most of the transparency range, and a damage threshold that is higher than either AGS or AGSe. The crystal is negative biaxial, having an angle between the optic axis of ~65° at 1064 nm. For 1064 nm pumping, Type I phase matching in the X-Z plane can generate an idler tunable from 2128 nm to 10 µm with an angular tuning of only 12.8°. In the X-Y plane, Type II phase-matching exists with a short wavelength limit of 2.52 µm, but the nonlinear coefficient is ~50% higher than in the X-Z plane. A tuning range from 5 to 10 µm is covered in this plane with an angular tuning of 10.9°. For our first study, we chose a crystal cut in the X-Y plane at φ= 38.9° measuring 6x6x12 mm^3 long, having quarter wave AR coating centered at 5.4 µm.

For a 20 ps pulse at 1064 nm, we found the surface damage threshold to be near 1 J/cm^2. Specifically, we observed immediate surface clouding with a pump energy of 15 mJ/pulse. This permitted us to safely pump the LIS OPA stage with 12 mJ/pulse. Although AGS can be pumped with this energy, we have observed a slower surface clouding effect (on the time scale of a few weeks) at this pump energy. In fact, slow surface clouding was observed for AGS at half this pump energy. We are currently investigating LIS for this slower surface clouding effect. It is likely that the specific damage threshold and time scale until surface damage occurs is very sensitive to the pump beam spatial energy profile. A detailed comparison of the damage thresholds of LIS and AGS is given is section 10 of reference 8. In our experiment, the mid-IR output measured at this pumping level (12 mJ/pulse) is shown in Figure 2. At 1850 cm^{-1}, the output of 0.35 mJ corresponds to conversion of nearly 15% of the 1064 nm pump.

A second crystal in tandem oriented for walk-off compensation did not result in a significant increase in the conversion efficiency. With the type of phase matching

employed, this second crystal would need to be cut from an adjacent crystal quadrant (i.e., φ= -38.9 or +141.1°) in order to have the correct sign for the nonlinear coefficient[20] and this could not be verified for the crystal pairs we tried.

Phase-matching is also possible in LIS with propagation outside of the principal planes. The main advantage of an out of plane cut is an increase in the nonlinear coefficient caused by the rotation of the polarization directions from the plane of propagation containing the Z axis. This rotation is a result of the biaxial nature of the crystal and it can be quite large at propagation directions near the optic axis. In the formula for the second-order nonlinearity, this rotation angle (δ) couples the tensor element d_{33} (=-16(+/- 25%) pm/V)[8] to the total nonlinear coefficient. This contribution can increase in the calculated nonlinear coefficient by a factor of two. We investigated a crystal cut at θ= 59.9, φ= 20.5° measuring 7x7x12 mm^3. This angle was far from the optimum cut of θ= 65, φ= 30°, so the rotation angle of the crystal needed to generate the same wavelengths as the on-axis cut reported above was quite large, resulting in some loss in 'clear aperture' and efficiency. The results are shown in figure 3 (1064 nm pump energy was 10 mJ/pulse). This out of plane cut can cover the full tuning range from 2.128 to 10 μm with an internal angle change of 15.7°.

Peptide Synthesis and Experimental Details

Peptide synthesis and experimental details, such as PBS buffer type and SFG sample geometry are identical to our previous publication[17] (the one exception being the use of substrate: fused silica is not transparent in the mid infrared. Therefore, calcium fluoride was used in this study). The sequence of the peptide studied here (named LK_{14}) is Ac-LKKLLKLLKKLLKL-NH_2. Details concerning SFG vibrational spectroscopy are

available in the literature.[21-25] The spectrum presented here are is in the *ssp* polarization combination (SFG, visible, and IR, respectively). The data in Figure 4 was taken with the LIS crystal cut in the X-Y plane at φ= 38.9° measuring 6x6x12 mm^3 long, having quarter wave AR coating centered at 5.4 μm.

Results and Discussion

The SFG spectrum of LK_{14} adsorbed from PBS buffer at the d_8-PS/buffer interface is shown in Figure 4. The vibrational mode observed around 1655 cm^{-1} is assigned to the Amide I mode of the peptide backbone (it should be noted here that the signal-to-noise ratio in Figure 4 is less than that published by the Chen group[11-14]. This is likely due to the fact that we are far away from the sum frequency, visible, and infrared critical angle. Although this results in lower signal-to-noise ratio, it can simplify the interpretation of the spectrum[23]). It is well accepted in infrared, Raman, and more recently SFG studies that a Amide I mode at 1650 cm^{-1} can be assigned to an α-helix.[10] Additionally, it has been established that the LK_{14} peptide is an α-helix in solution under these experimental conditions.[15, 18] Therefore, this spectrum could be interpreted as showing that the LK_{14} has maintained its α-helical structure upon adsorption. However, the vibrational energy of a random coil has a wide range; certainly, it is possible for a random coil to also have a Amide I frequency of 1655 cm^{-1}. Additionally, interactions with a solid surface can blue- or red-shift vibrational modes. It is well accepted that the local environment of a molecule can have a strong affect on its vibrational energy.[26] For example, if the LK_{14} peptide is a random coil, the frequency of the Amide I mode could be anywhere in the range 1600-1700 cm^{-1}. Even if the vibrational frequency of the random coil is not ~1655 cm^{-1} in solution, it could be shifted to this energy via

interactions with the surface. Therefore, a definitive assignment at this time is not possible. We are currently working on methods to make this assignment clear.[27]

Conclusions

We have developed a new OPA based on LIS. This allows for the production of infrared light with wavelength between 1500 cm^{-1} and 2000 cm^{-1}. This LIS OPA provides more power and better beam quality than either AGS or AGSe. This new OPA has been used to measure the Amide I vibrational mode of a model peptide, LK_{14}. We have found that the frequency of the Amide I mode of this peptide at the hydrophobic d_8-PS/buffer interface to be centered around 1655 cm^{-1}, possibly implying an α-helical structure on this surface.

Acknowledgements

This work was supported by the Director, Office of Science, Office of Basic Energy Sciences, Materials Sciences and Engineering Division, of the U.S. Department of Energy under Contract No. DE-AC02-05CH11231. Additional support was provided by the NIH through grant R21EB005262. We would like to thank William K. Browne and Prof. Phillip Geissler for insightful discussions.

Online Supporting Information Available

The raw, unnormalized data that comprises Figure 3 is available as an online supplement.

References

1. D. G. Castner and B. D. Ratner, Surf. Sci. **500**, 1-3, 28 (2002).
2. B. Kasemo, Curr. Opin. Solid State & Mat. Sci. **3**, 451 (1998).
3. G. A. Somorjai, R. L. York, D. Butcher, and J. Y. Park, Phys. Chem. Chem. Phys. **9**, 3500 (2007).
4. *Proteins at Interfaces II: Fundamentals and Applications* (American Chemical Society, Washington, D. C., 1995), 1st ed.
5. X. Y. Chen, M. L. Clarke, J. Wang, and Z. Chen, Int. J. Mod. Phys. B **19**, 4, 691 (2005).

6. J. Wang, M. L. Clarke, X. Y. Chen, M. A. Even, W. C. Johnson, and Z. Chen, Surf. Sci. **587**, 1-2, 1 (2005).
7. R. L. York, W. K. Browne, P. L. Geissler, and G. A. Somorjai, Isr. J. Chem. **47**, 1, 51 (2007).
8. S. Fossier, S. Salaun, J. Mangin, O. Bidault, I. Thenot, J. J. Zondy, W. Chen, F. Rotermund, V. Petrov, P. Petrov, J. Henningsen, A. Yelisseyev, L. Isaenko, S. Lobanov, O. Balachninaite, G. Slekys, and V. Sirutkaitis, J. Opt. Soc. Am. B **21**, 11, 1981 (2004).
9. L. Isaenko, I. Vasilyeva, A. Yelisseyev, S. Lobanov, Y. Malakhov, L. Dovlitova, J. J. Zondy, and I. Kavun, J. Cryst. Growth **218**, 313 (2000).
10. S. Krimm and J. Bandekar, Adv. Prot. Chem. **38**, 181 (1986).
11. J. Wang, M. A. Even, X. Y. Chen, A. H. Schmaier, J. H. Waite, and Z. Chen, J. Am. Chem. Soc. **125**, 9914 (2003).
12. J. Wang, X. Y. Chen, M. L. Clarke, and Z. Chen, Proc. Natl. Acad. Sci. U. S. A. **102**, 4978 (2005).
13. X. Y. Chen, J. Wang, J. J. Sniadecki, M. A. Even, and Z. Chen, Langmuir **21**, 2662 (2005).
14. X. Y. Chen and Z. Chen, Biochim. Biophys. Acta, Biomembr. **1758**, 9, 1257 (2006).
15. W. F. Degrado and J. D. Lear, J. Am. Chem. Soc. **107**, 25, 7684 (1985).
16. J. R. Long, N. Oyler, G. P. Drobny, and P. S. Stayton, J. Am. Chem. Soc. **124**, 22, 6297 (2002).
17. O. Mermut, D. C. Phillips, R. L. York, K. R. McCrea, R. S. Ward, and G. A. Somorjai, J. Am. Chem. Soc. **128**, 11, 3598 (2006).
18. R. L. York, O. Mermut, D. C. Phillips, K. R. McCrea, R. S. Ward, and G. A. Somorjai, J. Phys. Chem. C **111**, 25, 8866 (2007).
19. R. W. Boyd, *Nonlinear Optics* (Academic Press, San Diego, 2003), 2nd ed.
20. D. J. Armstrong, W. J. Alford, T. D. Raymond, A. V. Smith, and M. S. Bowers, J. Opt. Soc. Am. B **14**, 2, 460 (1997).
21. H. F. Wang, W. Gan, R. Lu, Y. Rao, and B. H. Wu, Int. Rev. Phys. Chem. **24**, 2, 191 (2005).
22. X. Wei, S. C. Hong, X. W. Zhuang, T. Goto, and Y. R. Shen, Phys. Rev. E **62**, 4, 5160 (2000).
23. P. B. Miranda and Y. R. Shen, J. Phys. Chem. B **103**, 17, 3292 (1999).
24. X. Zhuang, P. B. Miranda, D. Kim, and Y. R. Shen, Phys. Rev. B **59**, 19, 12632 (1999).
25. A. G. Lambert, P. B. Davies, and D. J. Neivandt, Appl. Spectrosc. Rev. **40**, 2, 103 (2005).
26. J. D. Smith, R. J. Saykally, and P. L. Geissler, J. Am. Chem. Soc. **129**, 45, 13847 (2007).
27. J. Wang, S. H. Lee, and Z. Chen, J. Phys. Chem. B **112**, 7, 2281 (2008).

Figure Captions:

Figure 1. Schematic of the OPG/OPA. Briefly, a pump Nd:YAG laser sends light at 1064 nm into the OPG/OPA. This light is split into two beams (Beam I and Beam II). Beam I is sent into a KTP crystal, where it is frequency doubled to 532 nm. This beam is split into two (Beam Ia and Ib). Beam Ia is used as the visible (VIS) beam for our SFG experiment. Beam Ib is sent into a set of two angle tunable KTP crystals, whereby two more beams are created (Beams 2a and 2b) by a process called optical parametric generation. Beam 2a (the "signal") is light at ca. 900 nm, and Beam 2b (the "idler") is light at ca. 1300 nm, whereby the exact frequency of Beams 2a and 2b is determined by the angles of the KTPs relative to the incoming Beam Ib. Beam 2a is dumped, and Beam 2b is sent to a second set of non-linear crystals (LIS). Here, Beam II and Beam 2b (the idler from stage 1 becomes the signal in stage 2) are mixed in the LIS crystals, and light at the difference frequency (between the two incoming beams) is created. This light (the idler from LIS) has a tunable wavelength between 5000 nm (or less) and 7000 nm (or more) and becomes the infrared (IR) for our SFG experiments.

Figure 2. Infrared intensity output of LIS OPA (φ = 38.9° measuring 6x6x12 mm^3 long, having quarter wave AR coating centered at 5.4 μm). The intensity of the 1064 nm pump was 12 mJ/pulse.

Figure 3. Infrared intensity output of LIS OPA (θ= 59.9, φ= 20.5° measuring 7x7x12 mm^3, having quarter wave AR coating centered at 5.4 μm). The intensity of the 1064 nm pump was 10 mJ/pulse. Since two different energy meters with slightly different sensitivities were used to measure the IR intensity between 1500-2100 cm^{-1}, 2100-3100 cm^{-1}, and 3100-4000 cm^{-1}, the data were normalized such that the IR intensities at 2100

cm^{-1} and 3100 cm^{-1} were equal. See the supporting information for the raw, unnormalized data.

Figure 4. The Amide I SFG spectrum of 0.15 mg/mL (bulk solution concentration) LK_{14} in PBS buffer (■) at the deuterated polystyrene/solution interface and the SFG spectrum of the deuterated polystyrene/solution interface (.). The location of the Amide I mode centered at 1655 cm^{-1} is characteristic of an α-helical peptide.

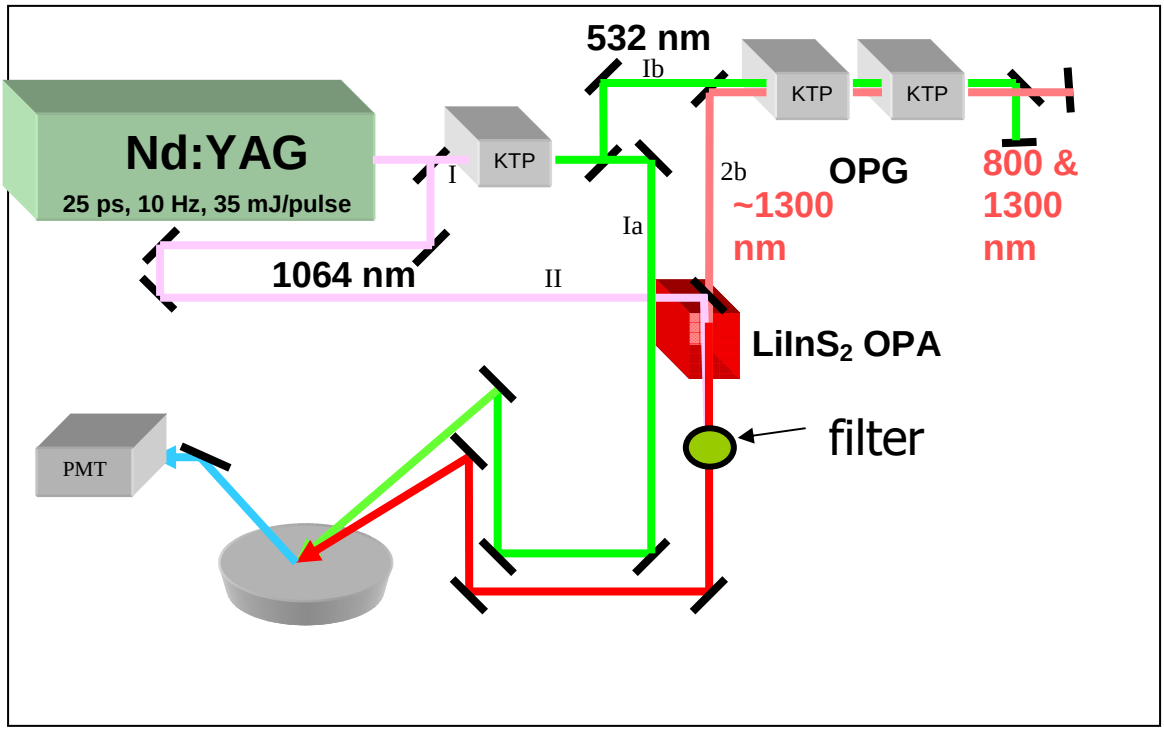
532 nm
Ib
KTP
KTP
Nd:YAG
25 ps, 10 Hz, 35 mJ/pulse
I
KTP
2b
OPG
~1300
nm
800 &
1300
nm
Ia
1064 nm
II
LiInS2 OPA
filter
PMT

Figure 1.

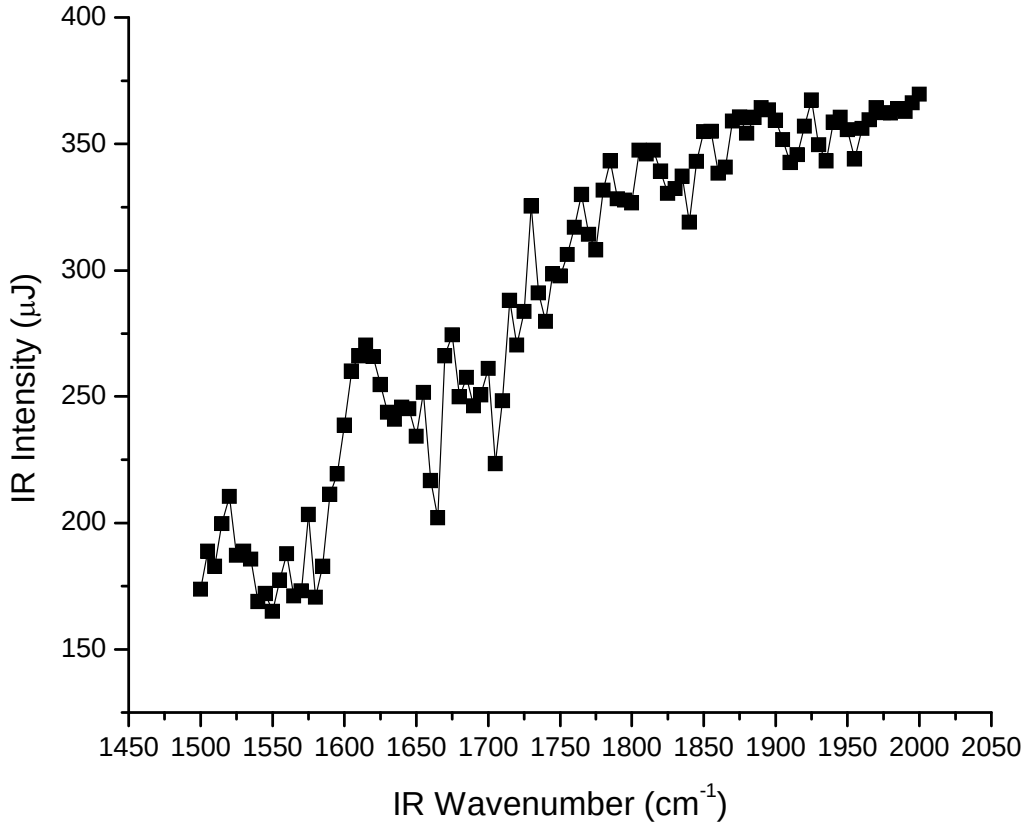
400
350
300
250
200
150
IR Intensity (μJ)
1450 1500 1550 1600 1650 1700 1750 1800 1850 1900 1950 2000 2050
IR Wavenumber (cm-1)

Figure 2.

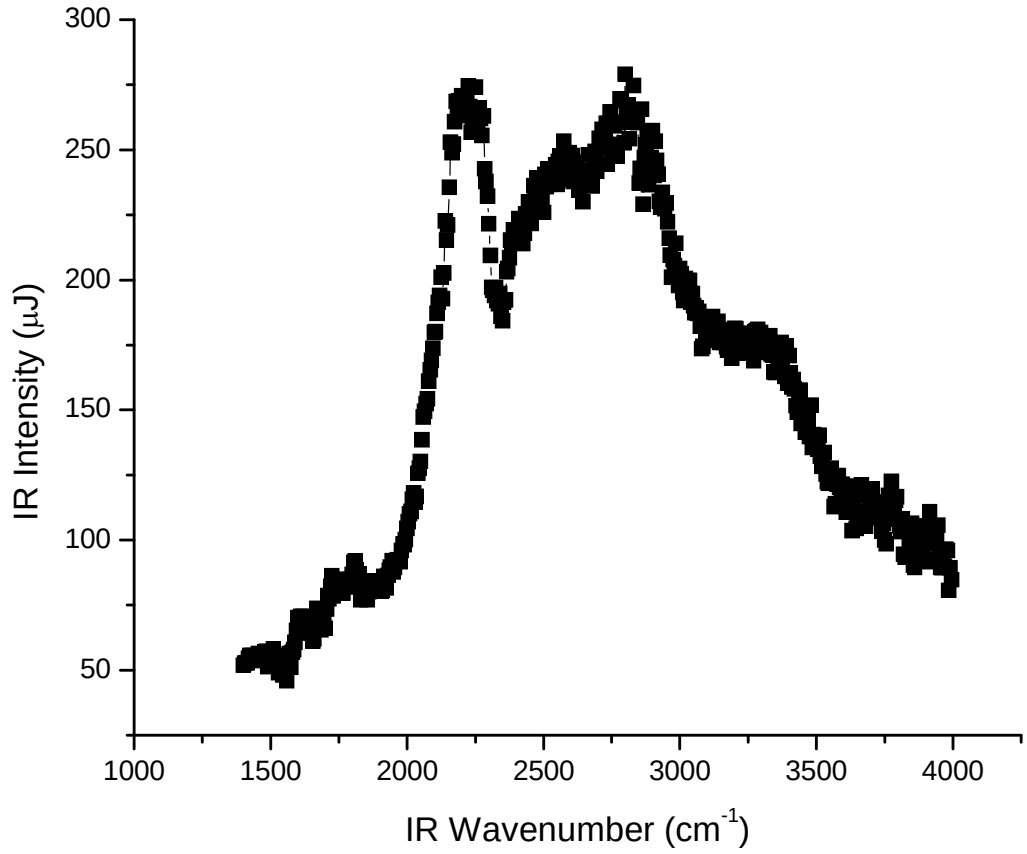
300
250
200
150
100
50
IR Intensity (μJ)
1000
1500
2000
2500
3000
3500
4000
IR Wavenumber (cm-1)

Figure 3.

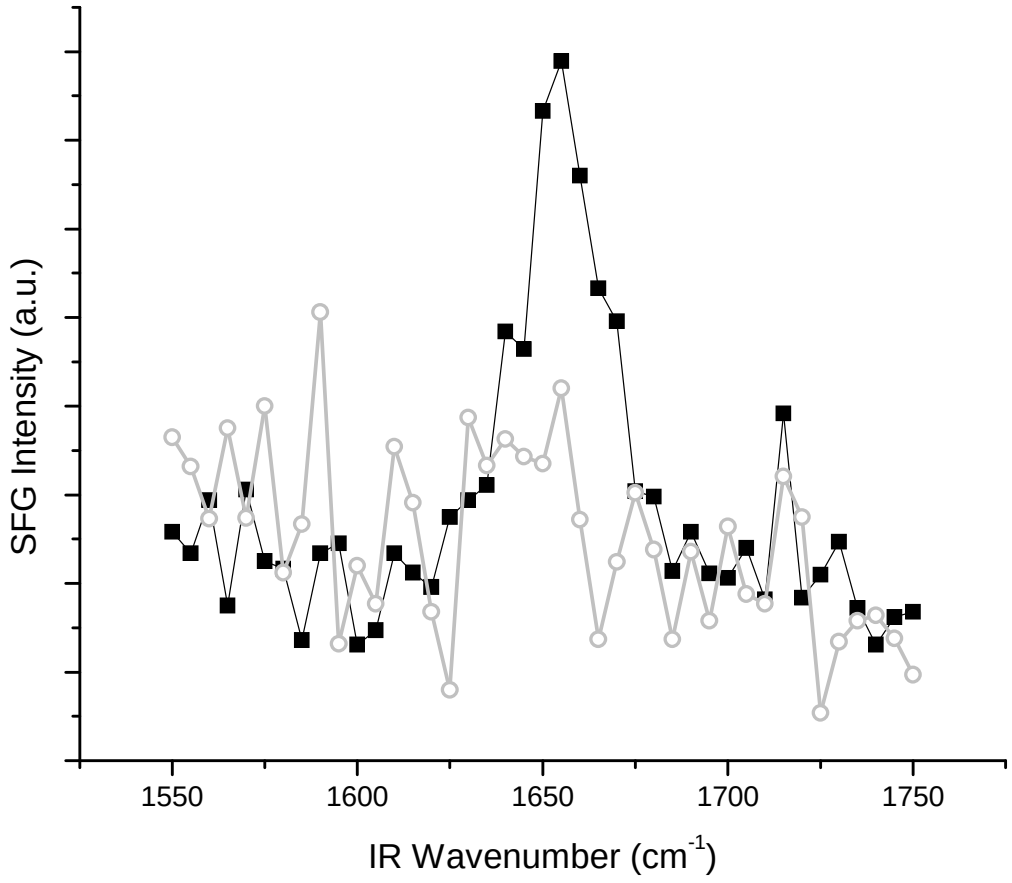

Figure 4.